Precambrian Research 351 (2020) 105931

Contents lists available at ScienceDirect

Precambrian Research

journal homepage: www.elsevier.com/locate/precamres

The terminal Ediacaran tubular fossil *Cloudina* in the Yangtze Gorges area of South China

Dandan Liang[a], Yaoping Cai[a,*], Morrison Nolan[b], Shuhai Xiao[b,*]

[a] State Key Laboratory of Continental Dynamics, Shaanxi Key Laboratory of Early Life and Environments, Department of Geology, Northwest University, Xi'an 710069, China

[b] Department of Geosciences, Virginia Tech, Blacksburg, VA 24061, USA

ARTICLE INFO

Keywords:
Ediacaran
Biomineralization
Cloudina
Sinotubulites
Dengying Formation
South China

ABSTRACT

The advent of biomineralizing metazoans in the terminal Ediacaran Age (ca. 550–539 Ma) represents a remarkable biological innovation in the history of life. As a poster child of this evolutionary episode, *Cloudina* is widely regarded as a weakly biomineralizing tubular fossil with a global distribution. Therefore, *Cloudina* can both inform the evolution of animal biomineralization and facilitate terminal Ediacaran stratigraphic correlation. However, this key taxon has not been fully described from the Yangtze Gorges area of South China, where classical terminal Ediacaran strata have been investigated extensively by paleontologists, stratigraphers, and geochemists. Here we document an assemblage of three-dimensionally silicified tubular fossils from siliceous dolostone of the terminal Ediacaran Baimatuo Member of the Dengying Formation in the Yangtze Gorges area, western Hubei Province, South China. The Baimatuo assemblage consists of *Sinotubulites* (which has been previously known in the Baimatuo Member), as well as *Cloudina* (including *C. ningqiangensis*, *C. hartmannae*, *C.* cf. *carinata*, and *C.* sp. indet.) and other unnamed tubular forms. This discovery adds to the diversity of early biomineralizing metazoans in the Yangtze Gorges area and facilitates the biostratigraphic correlation of the *Cloudina–Sinotubulites* co-occurrence assemblage in terminal Ediacaran strata.

1. Introduction

Cloudina is arguably the best known Precambrian biomineralizing animal fossil (Cortijo et al., 2015a; Grant, 1990; but see Yang et al., 2020). Although it may extend into the early Cambrian (Yang et al., 2016; Zhu et al., 2017; Zhuravlev et al., 2012), *Cloudina* is globally found in terminal Ediacaran strata and its first appearance datum is a promising biostratigraphic marker to define the terminal Ediacaran Stage (Xiao and Narbonne, 2020). Additionally, *Cloudina* tends to co-occur with other characteristic terminal Ediacaran fossils and thus has the potential to aid global biostratigraphic correlation through cross-referencing to different taxa. For example, it co-occurs with (1) *Sinotubulites* in the Beiwan Member of the Dengying Formation in southern Shaanxi Province of South China (Cai et al., 2019) and in the Ibor Group in Iberia (Cortijo et al., 2015b), (2) *Corumbella* in the Corumbá Group of western Brazil (Walde et al., 2019) and in the Tagatiyá Guazú Formation of Paraguay (Warren et al., 2017), and (3) *Namacalathus* in the Nama Group of southern Namibia (Wood and Curtis, 2015), the Ara Group in Oman (Amthor et al., 2003), the Byng Formation of the Miette Group in the Canadian Rocky Mountains (Hofmann and Mountjoy, 2001), the Tagatiyá Guazú Formation in Paraguay (Warren et al., 2017), and possibly the Raiga Formation in western Siberia (although the Siberian *Namacalathus* specimens are much smaller than those from other continents; Grazhdankin et al., 2015; Kontorovich et al., 2008). In South China, three-dimensionally silicified specimens of *Sinotubulites* were first reported from the Baimatuo Member of the Dengying Formation in the Yangtze Gorges area (Chen et al., 1981), and three-dimensionally phosphatized specimens of *Cloudina* and *Sinotubulites* were later reported from the Dengying Formation in the Ningqiang area of southern Shaanxi Province (Hua et al., 2000; Zhang et al., 1992). Recently, Chen et al. (2016) illustrated *Cloudina* specimens in thin sections from the Shibantan Member of the Dengying Formation in the Yangtze Gorges area. Following Chen et al. (2016), in this paper we document and describe three-dimensionally silicified *Cloudina* fossils, along with *Sinotubulites* and other tubular fossils, from the Baimatuo Member of the Dengying Formation in the Yangtze Gorges area, Hubei Province, South China. The new discovery demonstrates the occurrence of the *Cloudina–Sinotubulites* assemblage in the Yangtze Gorges area and adds new data to terminal Ediacaran biostratigraphy and the early evolution of animal biomineralization.

* Corresponding authors.
E-mail addresses: yaopingcai@nwu.edu.cn (Y. Cai), xiao@vt.edu (S. Xiao).

https://doi.org/10.1016/j.precamres.2020.105931
Received 21 April 2020; Received in revised form 30 August 2020; Accepted 1 September 2020
Available online 11 September 2020

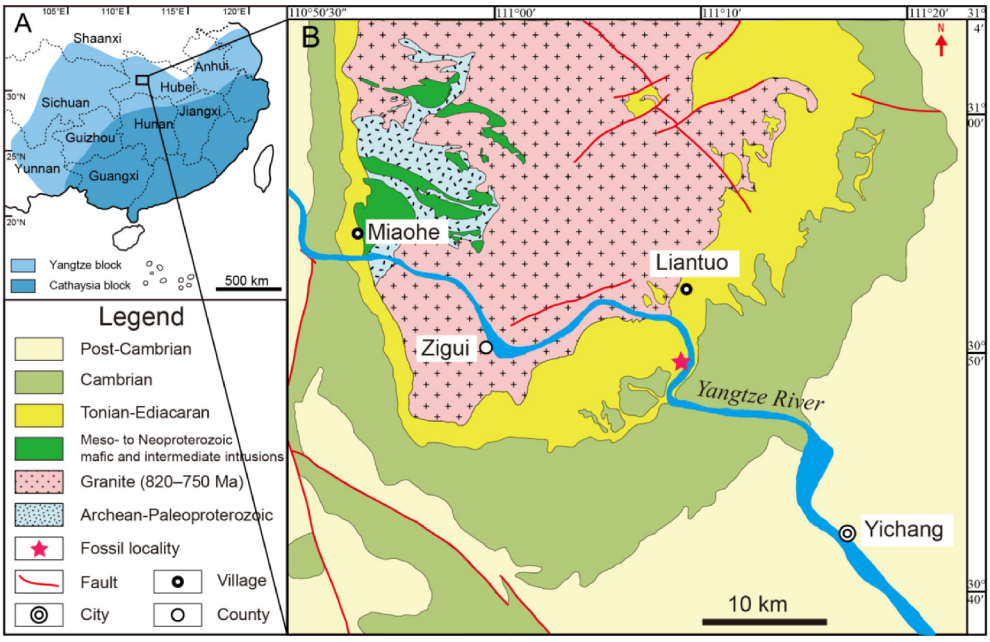

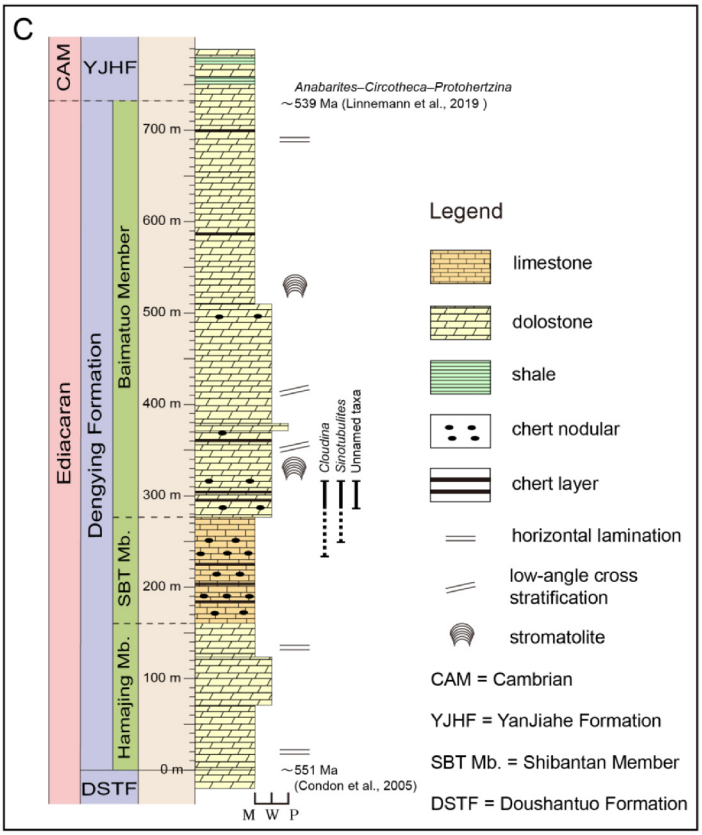

Fig. 1. Geological map and fossil locality. (A) Major tectonic units of South China, including the Yangtze and Cathaysia blocks. (B) Geological map of the Yangtze Gorges area (rectangle in A), showing the fossil locality at the Baimatuo section (red star) near Yichang, Hubei Province, South China. Modified from Zhao et al. (2013). (C) Stratigraphic column of the Ediacaran Dengying Formation at the Baimatuo section. Previous studies have shown that *Sinotubulites* occurs in the upper Shibantan and lower Baimatuo members (Chen et al., 1981, 2014) and that *Cloudina* is present in the middle Shibantan Member (Chen et al., 2016), and this paper reports the discovery of *Cloudina* from the lower Baimatuo Member. M = Mudstone; W = Wackestone; P = Packstone. (For interpretation of the references to color in this figure legend, the reader is referred to the web version of this article.)

2. Stratigraphic setting and fossil material

The fossil locality (Baimatuo section; Fig. 1A and B; GPS: 30°49′2″N, 111°9′59″E) is located in the Yangtze Gorges area of the Yangtze Block, ca. 20 km northwest of the city of Yichang. The Ediacaran System in the Yangtze Gorges area consists of the Doushantuo Formation and the overlying Dengying Formation, which is unconformably overlain by the basal Cambrian Yanjiahe Formation (Fig. 1C). In this area, the Dengying Formation is dominated by a suite of marine carbonates that can be sub-divided into three members—the Hamajing Member dolostone (Fig. 2A and B), the Shibantan Member limestone (Fig. 2C and D), and the Baimatuo Member dolostone (Fig. 2E–H) in ascending order. A detailed description of the lithostratigraphy of the Dengying Formation in this area can be found in Meyer et al. (2014) and Ding et al. (2019). The focus of this study is the Baimatuo Member, which is characterized by light gray, thick-bedded dolostone intercalated with chert beds or nodules (Fig. 2E and F). Dissolution vugs, columnar stromatolites (Fig. 2G), low-angle trough cross stratification (Fig. 2H), and horizontal lamination (Fig. 2E and F) are present in the Baimatuo Member, attesting to a peritidal depositional environment (Meyer et al., 2014).

Specimens of *Cloudina*, *Sinotubulites*, and other tubular fossils were collected from the lower part of the Baimatuo Member (Fig. 1C). The

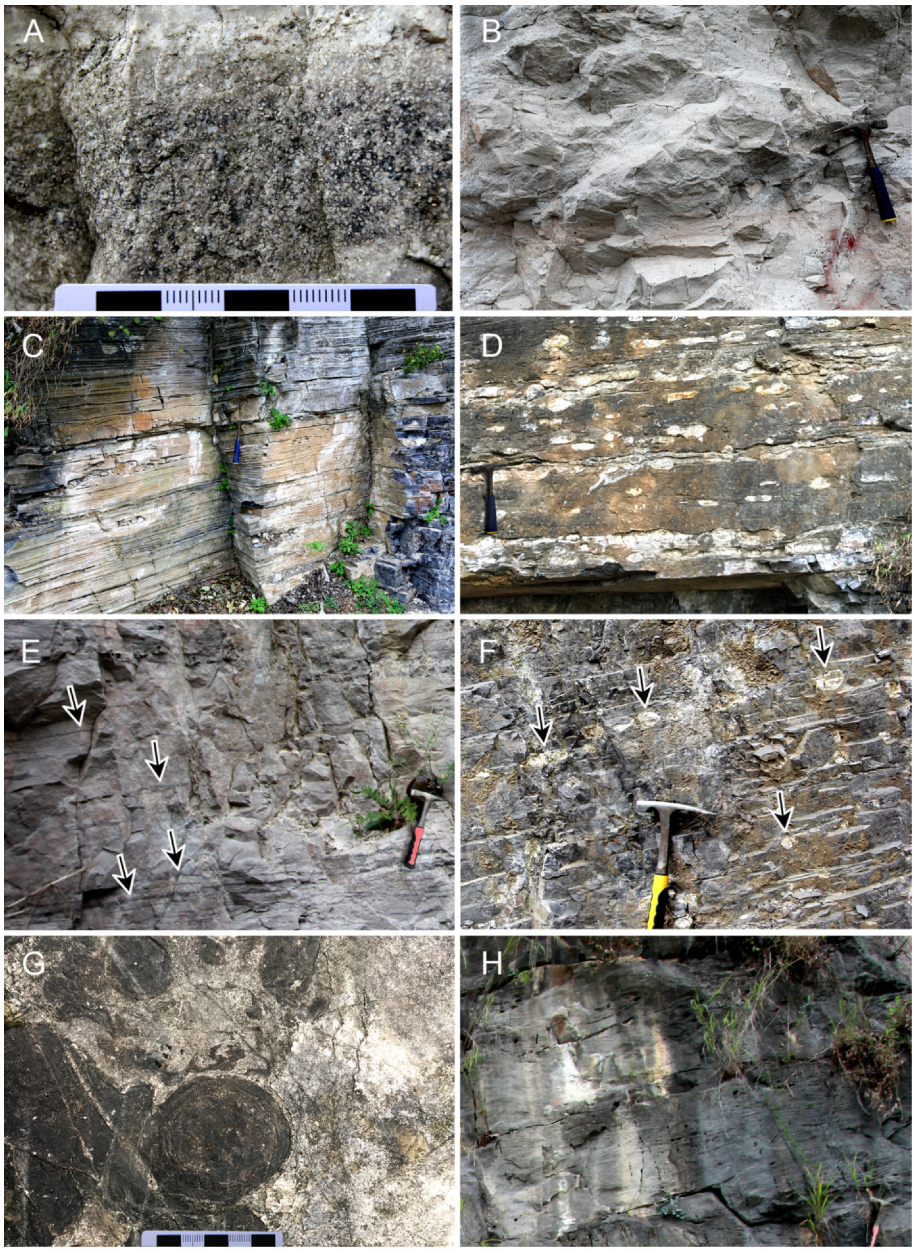

Fig. 2. Field photographs of lithology and sedimentary structures of the Dengying Formation. All photographs were taken along a roadcut on the southern bank of the Yangtze River between the Nantuo and Baimatuo villages. (A) "Grapestone" or void-filling botryoids in the lower Hamajing Member. Although superficially resemble oolite, the sample consists of void-filling botryoids and pisoliths forming near subaerial exposure surfaces. See Fig. 3B of Cai et al. (2010) and Fig. 2a of Cui et al. (2019) for similar structures in the equivalent Algal Dolomite Member of the Dengying Formation in southern Shaanxi Province. Black bar represents 1 cm. (B) Light gray, thick-bedded dolostone in the upper Hamajing Member. (C–D) Dark gray, thin-bedded limestone with chert layers and nodules (light-colored lenticular structures in D) in the upper Shibantan Member. (E–F) Gray, thin- to medium-bedded, siliceous dolostone with chert layers (black arrows in E) and nodules (light-colored lenticular structures denoted by arrows in F) in the lower Baimatuo Member. Tubular fossils described in this paper were collected from this stratigraphic interval. (G) Bedding surface view of columnar stromatolites in the Baimatuo Member. (H) Low-angle trough cross stratification in dolostone in the Baimatuo Member. Rock hammer 28 cm.

fossil specimens are secondarily silicified and occur abundantly on bedding surfaces of weathered dolostone (Figs. 3A, 4A, 5A). Due to their resistance to weathering, fossils were exposed on weathered bedding surfaces. Silicification has obscured the morphological details in most specimens. Nonetheless, well preserved specimens can occasionally be found on bedding planes. Some naturally exposed specimens were photographed as they were found (Figs. 3 and 4) or after brief treatment with 10% acetic acid to remove debris (Figs. 5, 8A, 9), others were extracted after acid digestion in 15% acetic acid for one week (Figs. 6 and 7), and selected specimens were cut into thin sections for petrographic observation (Fig. 8B–M). Specimens illustrated in this paper are reposited at the Department of Geology, Northwest University (GEONWU), Xi'an, China.

3. Fossil description

Description of *Cloudina* fossils follows the terminology of Cai et al. (2017), and fossil measurements are presented in Table 1. The great majority of the Baimatuo *Cloudina* fossils in our collection are silicified and are preserved with their long axis roughly parallel to or at low angles with the bedding plane. Most *Cloudina* fossils are incompletely preserved, often with the apical end missing. However, the characteristic funnel-in-funnel tube construction (Cortijo et al., 2010; Hua et al., 2005) is easily seen (e.g., Figs. 3C, 4A–D, 5B). Most of the preserved tubes are straight and taper slightly toward the presumed apical end, but some of them are slightly curved. Although the apertural rim of the constituent funnels is often broken or poorly preserved, the boundary between adjacent funnels can be clearly seen (Fig. 4B, D).

The following *Cloudina* species can be recognized in our collection: *C. ningqiangensis*, *C. hartmannae*, *C.* cf. *carinata*, and *C.* sp. indet. According to Cortijo et al. (2010) and Cai et al. (2017), the key diagnostic feature for distinguishing *C. ningqiangensis*, *C. hartmannae*, and *C. carinata* is the pattern of ornamentations on the exterior surface of the funnels, rather than the apertural and apical rims of the funnels, which occur in all *Cloudina* species. *C. ningqiangensis* is characterized by the absence of annulations on the funnels (i.e., funnels are smooth), and *C. hartmannae* by transverse and/or oblique annulations throughout the exterior surface of the funnels (Cai et al., 2017). *C. carinata* is

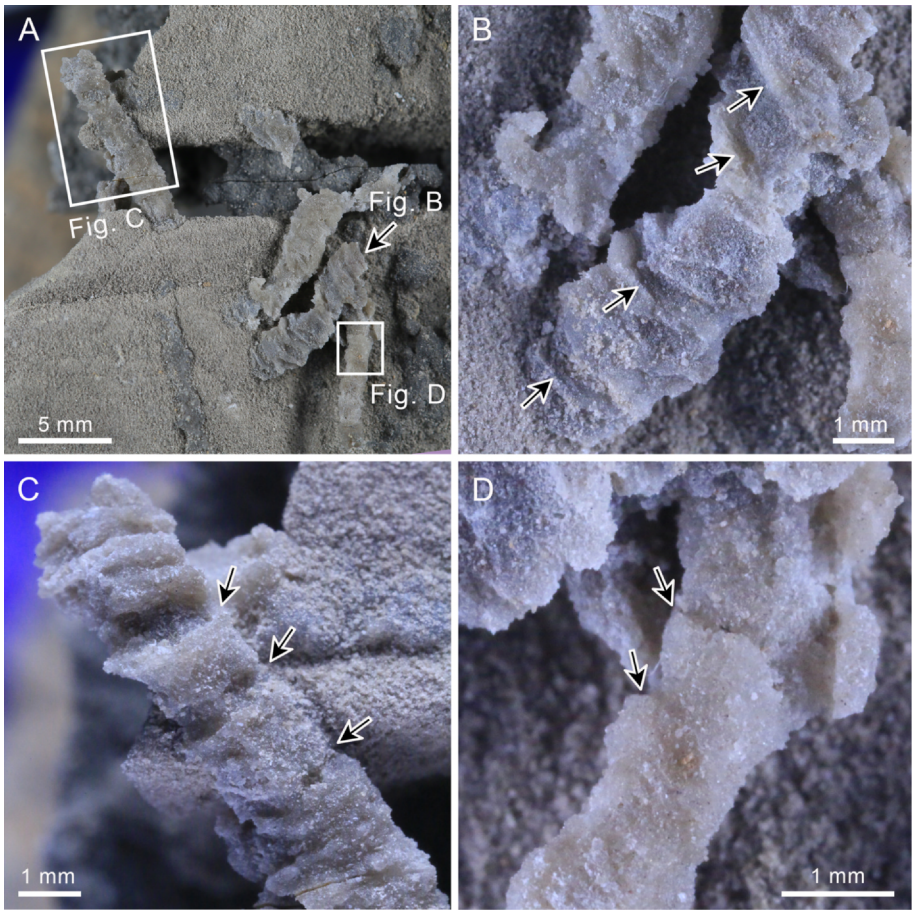

Fig. 3. Reflected light photographs of poorly preserved *Cloudina* and *Sinotubulites* specimens in siliceous dolostone beds of the terminal Ediacaran Baimatuo Member of the Dengying Formation at the Baimatuo section. (A) Bedding plane view of *Cloudina* and co-occurring *Sinotubulites* (black arrow). Labeled boxes and arrow mark specimens enlarged in (B–D). (B) Close up of *S. baimatuoensis*. Note characteristic transverse corrugations (black arrows) on the tube. (C) Close up of *C. ningqiangensis*. Note the poorly preserved "funnel-in-funnel" (black arrows) tube construction. (D) Close up of *C.* sp. indet. Note the "funnel-in-funnel" (black arrows) tube construction. Museum catalog numbers: B (GEONWU-2019-BST001-001), C (GEONWU-2019-BST001-002), D (GEONWU-2019-BST001-003).

characterized by longitudinal crests that occur on the exterior surface of the funnels (Cortijo et al., 2010). Specimens of *C. ningqiangensis* (e.g., Fig. 3C) are poorly preserved, 5.0–10.9 mm in length (mean = 8.1 mm, s.d. = 2.4 mm, n = 3), 0.6–1.4 mm in diameter at the narrower or adapical end (mean = 1.1 mm, s.d. = 0.3 mm, n = 3), and 1.6–2.4 mm in diameter at the wider or adapertural end (mean = 2 mm, s.d. = 0.3 mm, n = 3). The slightly thickened apertural rims of the funnels are occasionally preserved but no transverse annuli are present (Fig. 3C), suggesting a taxonomic identification with *C. ningqiangensis*. One specimen in our collection shows poor preservation of transverse to oblique annulations on the exterior surface of the funnels, and it can be identified as *C. hartmannae* (Fig. 4). The sparse occurrence of faintly visible transverse and oblique annulations in this specimen is probably related to its internal mold preservation, but it is possible that annulations were more prominent on the external surface of the funnels (see discussion in Cai et al., 2017). This specimen is 28.1 mm in length, 1.7 mm in diameter at the narrower (adapical) end, and 2.5 mm in diameter at the wider (adapertural) end. The slightly thickened apertural rims of the funnels are occasionally preserved with faint annuli (Fig. 4E). One poorly preserved specimen of *Cloudina* (Fig. 3D) is placed in an open nomenclature, *C.* sp. indet. It is 8.9 mm in length, 0.8 mm in diameter at the narrower (adapical) end, and 1.6 mm in diameter at the wider (adapertural) end. Finally, a tubular specimen in our collection is tentatively identified as *C.* cf. *carinata* (Fig. 5B). It is 27.4 mm in length, 2.3 mm in diameter at the narrower (adapical) end, and 4.2 mm in diameter at the wider (adapertural) end. It consists of a series of nested, more or less regularly spaced, and adaperturally flaring funnels. Some funnels appear to have longitudinal crests, a defining feature of *C. carinata*. Apertural rims are absent or poorly preserved. Compared with *C. carinata* from the Villarta Formation of the Ibor Group in Iberia (Cortijo et al., 2010) and the Tamengo Formation of the Corumbá Group in western Brazil (Adôrno et al., 2019), the funnels of the Baimatuo specimen are more irregularly spaced and have less prominent or poorly preserved apertural rims, highlighting its similarity to *Sinotubulites* as recognized by Cortijo et al. (2010).

Most *Sinotubulites* specimens in our collection can be identified as *S. baimatuoensis*. They are cylindrical tubes 2.5–19.4 mm in length (mean = 8.5 mm, s.d. = 4.8 mm, n = 11) and 1.0–2.5 mm in diameter (mean = 1.7 mm, s.d. = 0.4 mm, n = 11). *Sinotubulites* is characterized by a multi-layered cylindrical tube ("tube-in-tube" construction, Fig. 6E), with smooth inner layers (Fig. 6E) and irregularly corrugated outer layers (Figs. 3B, 6A–D) (Cai et al., 2015; Chen et al., 2008; Chen and Sun, 2001).

A bamboo-shaped cylindrical tubular fossil (Fig. 5C, specimen to the right) is placed in an open nomenclature. It is a slender, straight tube with regularly spaced transverse ridges. The specimen is incompletely preserved, 18 mm in length, and 1.6 mm in diameter. Spacing between transverse ridges is about 2.6 mm (mean = 2.6 mm, s.d. = 0.2 mm, n = 3). The specimen is somewhat similar to "agglutinated tubular fossils" from the Fore-Yenisei sedimentary basin in western Siberia (Fig. 7a in Grazhdankin et al., 2015) in that both have evenly spaced transverse ridges. Another unnamed specimen with slender, straight, cylindrical, tubular morphology is illustrated in Fig. 5D. It is 22.1 mm in length, 2.3 mm in diameter, and has irregular corrugations and oblique ridges. The irregular corrugations are somewhat similar to, but more sparsely distributed than, the wrinkles on the tests of *Sinotubulites*.

Finally, a number of incompletely preserved and relatively featureless tubular fossils were extracted from the Baimatuo Member using acid digestion methods (Fig. 7). These include conotubular fossil with poorly defined transverse annulations (Fig. 7A), cylindrical fossils with poorly defined transverse wrinkles (Fig. 7B), curved tubular fossils with poorly defined oblique wrinkles (Fig. 7C and D), and featureless tubular

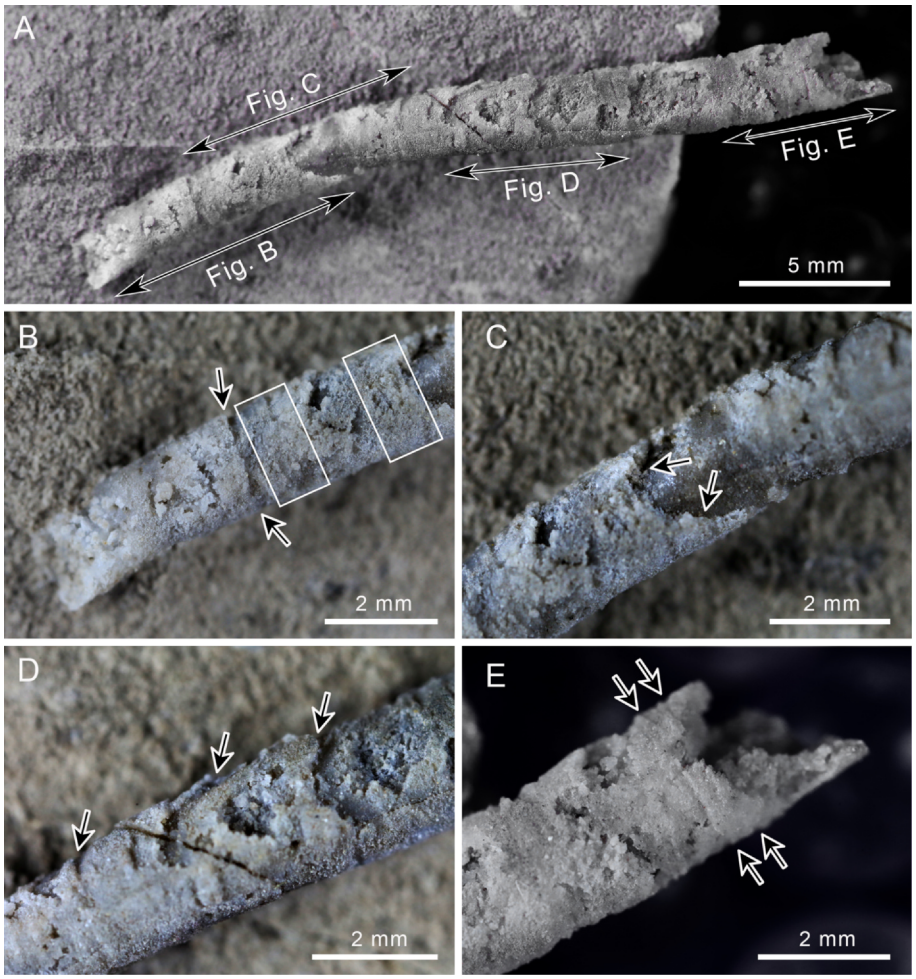

Fig. 4. Reflected light photographs of a well-preserved internal mold specimen of *Cloudina hartmannae* from the terminal Ediacaran Baimatuo Member of the Dengying Formation at the Baimatuo section. (A) Naturally exposed *C. hartmannae* specimen on a hand sample of weathered siliceous dolostone. The tube slightly tapers apically. Labeled double arrows mark areas enlarged in (B–E). (B–E) Close-up views of (A) showing key morphological features of *C. hartmannae*. Note the "funnel-in-funnel" construction (black arrows in B–C) formed by successively nested funnels (black arrows in D). Also note the apertural rim preserved as a couple of transverse annuli (black arrows in E). Poorly preserved transverse annulations can occasionally be seen on the main body of the funnels (rectangles in B). Museum catalog number: GEONWU-2019-BST002-001.

fossils (Fig. 7E and F).

4. Fossil preservation and paleoecology

To understand the taphonomy of the Baimatuo tubular fossils, selected specimens were prepared in thin sections and examined via petrographic microscopy, scanning electron microscopy (SEM), and X-ray energy dispersive spectroscopy (EDS) (Fig. 8). Two of the thin-sectioned specimens are slightly polygonal in transverse cross-sectional view (Fig. 8D), possibly reflecting the longitudinal crests of *Cloudina carinata* (Cortijo et al., 2010) or *Sinotubulites* (Cai et al., 2015). Cross polarized transmitted light microscopy shows that the tube walls are replicated with quartz and the tube interior is filled with dolomite (Fig. 8E and F). The dolomite crystals infilling the tube interior are larger than those in the sediment matrix (Fig. 8E and F), indicating that they formed as void-filling cement rather than internal sediment. The mineralogical difference between the tube wall and tube infill as inferred from petrographic observations is confirmed by backscattered electron SEM (Fig. 8G) and EDS elemental maps (Fig. 8H–M).

Based on the stratinomic features of the Baimatuo tubular fossils, we infer that they were transported, at least locally, prior to burial and fossilization. All specimens are preserved in parallel with the bedding plane with a slightly preferred orientation (Figs. 8A, 9) and their apex is never preserved intact. Thus, we infer that they must have been transported although they may not have been moved very far from where they lived (i.e., they were parautochthonously preserved).

We further infer that the Baimatuo tubes were likely buried with the animal inside and in episodic events (e.g., storm events). This inference is based on the observation that the tube interior is filled with sparry cement (Fig. 8E–F) rather than internal sediment. This observation indicates that the carcass inside the tube prevented the entry of sediment during burial in the taphonomic active zone.

Following burial, the tube walls were silicified and tube interior was filled with sparry carbonate cement. It is widely accepted that the tube walls of *Cloudina* and *Sinotubulites* were originally weakly biocalcified (Grant, 1990; Chen et al., 2008; Wood et al., 2017), although some researchers have argued that they were completely organic (Yang et al., 2020). Regardless, the predominantly siliceous composition of the Baimatuo tubular fossils indicates that the tube walls were secondarily silicified. Considering the abundance of chert layers and nodules in the host dolostone (Fig. 8A), we infer that fossil silicification in the Baimatuo Member may have been achieved by localized precipitation of authigenic silica during early diagenesis, perhaps related to a drop in local pH-Eh conditions driven by localized organic degradation (Xiao et al., 2010) and facilitated by elevated silica contents in Precambrian seawater (Maliva et al., 2005). Based on available data, it is not possible to determine whether the precipitation of sparry carbonate cement in tube interior occurred before or after tube wall silicification.

Because of post-mortem but pre-burial transportation, it is challenging to infer the paleoecology of the Baimatuo tubular fossils. Other workers have reconstructed *Cloudina* as an epibenthic tubular animal that anchored itself in the sediment (Warren et al., 2011; Cai et al., 2014), attached itself to small thrombolite domes (Warren et al., 2017), or constructed reef structures (Penny et al., 2014; Wood, 2016; Wood and Curtis, 2015). *Sinotubulites*, on the other hand, has been reconstructed as a procumbent epibenthic animal living on the ocean floor (Cai et al., 2015; Chen et al., 2008). The Baimatuo fossils are consistent with an epibenthic lifestyle in strong hydrodynamic

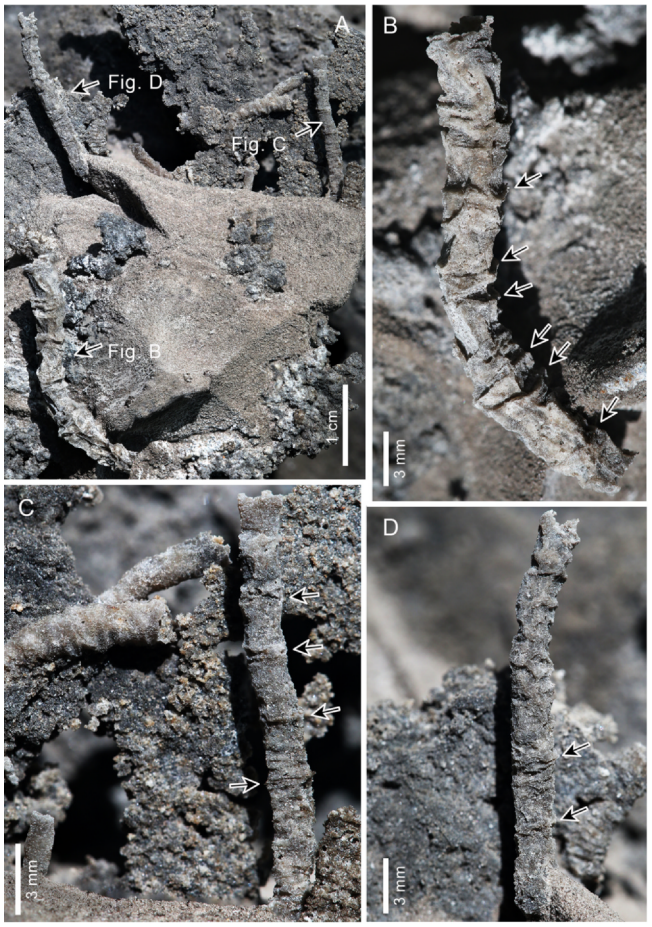

Fig. 5. Reflected light photographs of tubular fossils from the terminal Ediacaran Baimatuo Member of the Dengying Formation at the Baimatuo section. (A) Bedding plane view of a hand sample with multiple tubular fossils. Labeled arrows mark specimens enlarged in (B–D). (B) *C.* cf. *carinata* showing nested funnel-in-funnel construction and the characteristic longitudinal crests on the funnels. Apertural rims are indicated by arrows. (C) Two overlapping specimens on the left and a cylindrical specimen on the right with more or less evenly spaced transverse ridges (arrows). (D) Tubular fossil with irregular corrugations and oblique ridges (arrows). Museum catalog numbers: B (GEONWU-2019-BST003-001), C (GEONWU-2019-BST003-002), E (GEONWU-2019-BST003-003).

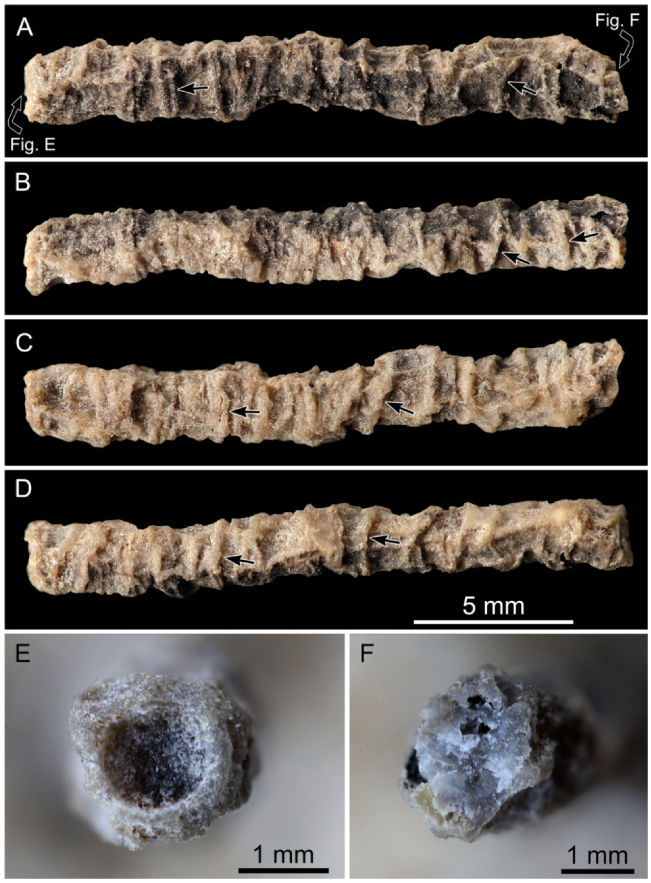

Fig. 6. Reflected light photographs of a well-preserved *Sinotubulites* specimen from the terminal Ediacaran Baimatuo Member of the Dengying Formation at the Baimatuo section. (A–D) are four views of the same specimen. Note transverse corrugations (black arrows) on the outer wall. (E–F) Cross-sectional views (see labeled arrows in A). Note that the multilayered tube wall is amalgamated into a single thick wall (lighter colored outer zone in E) due to silicification. The central lumen is filled with carbonate minerals (darker colored inner zone in E) or quartz (F). The outer wall is irregular in cross section, whereas the inner wall is circular. Museum catalog number: GEONWU-2019-BST001-006.

conditions (e.g., peritidal to subtidal environments). Other than that, the Baimatuo tubular fossils offer little insights into the paleoecology of *Cloudina* and *Sinotubulites* because of reworking and transportation (see also Mehra and Maloof, 2018).

5. Discussion

Together with the report of Chen et al. (2016), our study shows that silicified *Cloudina* fossils occur in the Shibantan and Baimatuo members of the Dengying Formation in the Yangtze Gorges area. Similarly, phosphatized *Cloudina* fossils are known from the Gaojiashan and Beiwan members of the Dengying Formation at the Lijiagou and Gaojiashan sections, respectively, in the Ningqiang area of southern Shaanxi Province (Cai et al., 2010, 2017); the Beiwan Member at the Lijiagou section was sometimes regarded as part of the upper Gaojiashan Member (Cai et al., 2014; Chen et al., 2008; Hua et al., 2005, 2007) but is here considered a separate lithostratigraphic unit overlying the Gaojiashan Member (Cai et al., 2010, 2017). *Cloudina* fossils from the Shibantan–Baimatuo and Gaojiashan–Beiwan members have similar tube sizes and show the diagnostic "funnel-in-funnel" tube construction, apertural rims on the funnels, and transverse annulations in some

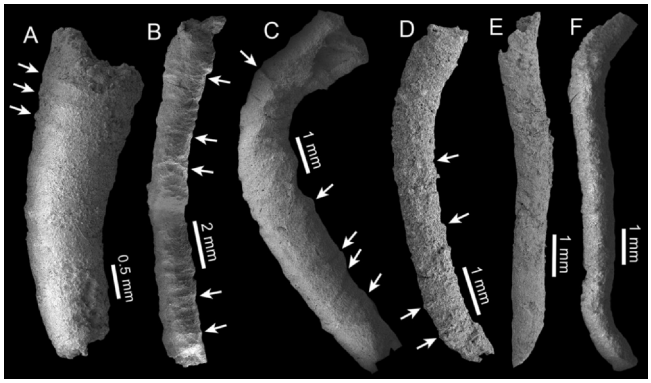

Fig. 7. Secondary electron microphotographs of taxonomically indeterminate tubular fossils extracted from the terminal Ediacaran Baimatuo Member of the Dengying Formation at the Baimatuo section. Arrows in (A–D) mark transverse and oblique corrugations or annulations. Museum catalog numbers: A (GEONWU-2019-YCSX-404-03), B (GEONWU-2019-YCSX-403-01), C (GEONWU-2019-YCSX-402-05), D (GEONWU-2019-YCSX-404-04), E (GEONWU-2019-YCSX-404-07), F (GEONWU-2019-YCSX-404-06).

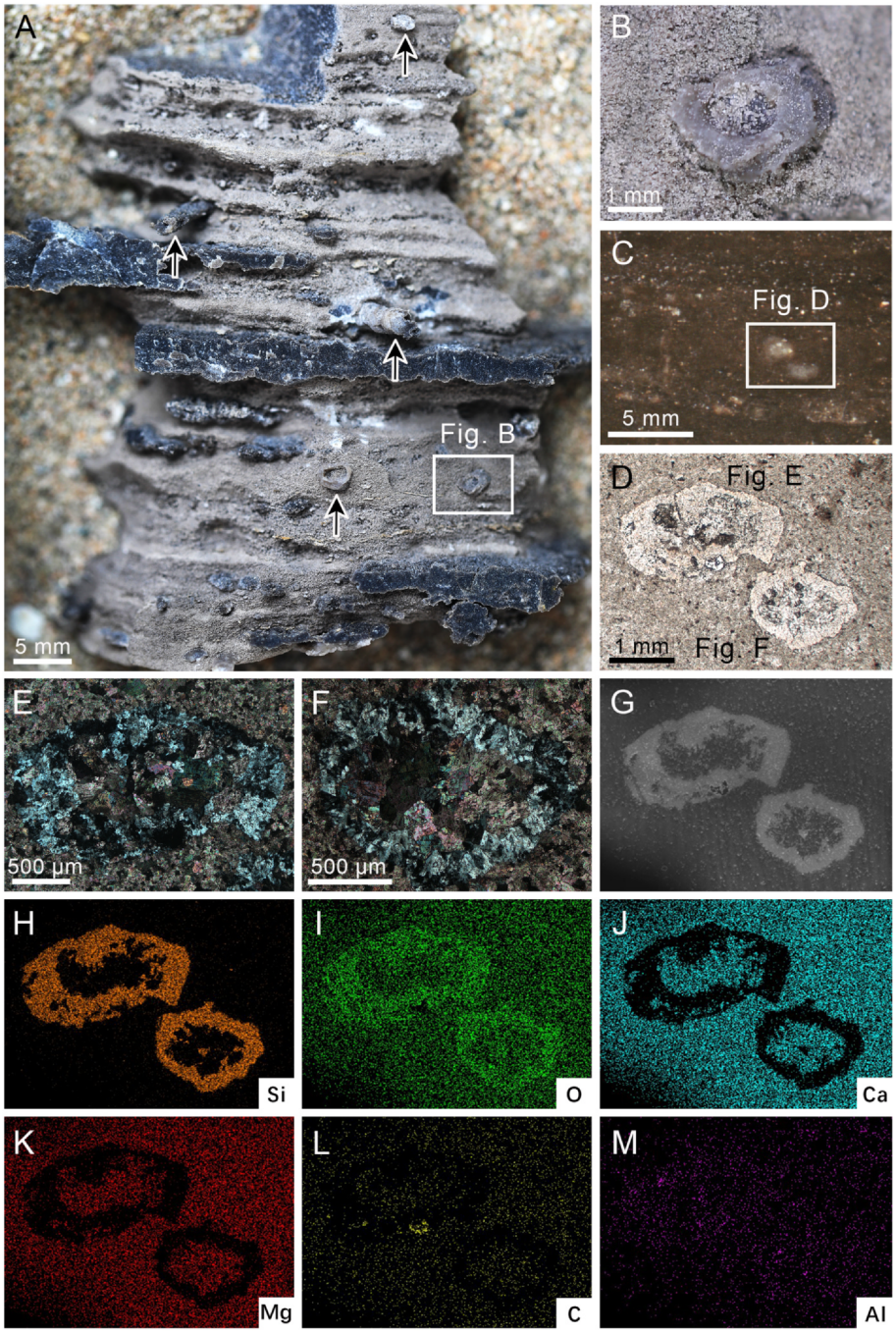

Fig. 8. Reflected light photographs of a hand sample (A–B), petrographic thin-section photomicrographs (C–F), backscattered electron (BSE) image (G), and X-ray energy dispersive spectroscopic (EDS) elemental maps (H–M), illustrating mineralogical and chemical compositions of Baimatuo tubular fossils. (A) Hand sample with multiple flat-lying specimens of tubular fossils (arrows). Silicified fossils are preferentially preserved in dolostone (lighter) rather than chert (darker) layers. (B) Transverse sectional view of a tubular fossil marked in A. (C) Reflected light photomicrograph of thin section showing transverse section of two tubular fossils. (D) Plane-polarized transmitted light photomicrograph of rectangled area in (C). (E–F) Cross-polarized transmitted light photomicrographs of the two specimens shown in D. Note the thin section is slightly thicker than standard thickness, as indicated by the birefringence color of quartz in the tube wall. (G) BSE image of the two specimens shown in D. (H–M) Elemental maps of Si, O, Ca, Mg, C, and Al, respectively. Museum catalog number: GEONWU-2019-BST004.

species (e.g., *Cloudina hartmannae*). These similarities indicate that, in South China, *Cloudina* is not restricted to the Ningqiang area and may have had a greater paleobiogeographic distribution even though it is thus far only known from the Yangtze Gorges and Ningqiang areas.

The co-occurrence of *Cloudina* and *Sinotubulites* presents a useful tool for biostratigraphic correlation in South China and globally. The *Cloudina–Sinotubulites* assemblage is now known to be present in the Beiwan Member of the Dengying Formation in the Ningqiang area (Cai et al., 2010, 2015, 2017; Zhang et al., 1992) and the Baimatuo Member of the Dengying Formation in the Yangtze Gorges area (this study); these two stratigraphic units have been correlated with each other based on independent lithostratigraphic data (Cai et al., 2011; Zhou and Xiao, 2007) and carbonate $\delta^{13}C$ chemostratigraphic data (Cui et al., 2019). In addition, Chen et al. (2014) indicated that *Sinotubulites* may be present in the Shibantan Member of the Dengying Formation in the Yangtze Gorges area, although they did not provide any illustrations or description; if confirmed, the *Cloudina–Sinotubulites* assemblage may also be present in the Shibantan Member, given the report of *Cloudina* from this stratigraphic unit (Chen et al., 2016). Considering the youngest detrital zircon age of 548 ± 8 Ma from the Gaojiashan Member in the Ningqiang area (stratigraphically older than the Beiwan Member; Cui et al., 2016) and the 551.1 ± 0.7 Ma ash from the Miaohe Member in the Yangtze Gorges area (stratigraphically older than the Baimatuo Member; Condon et al., 2005), the *Cloudina–Sinotubulites* assemblage in South China is likely younger than ca. 551 Ma. This estimate is consistent with recently reported radiometric ages from the Dengying Formation and stratigraphically equivalent units in South China. These ages include a 543.4 ± 3.5 Ma age from the Baimatuo Member in the Yangtze Gorges area (Huang et al., 2019), the 553.6 ± 2.7 Ma and 546.3 ± 2.7 Ma ages from the Jiucheng Member

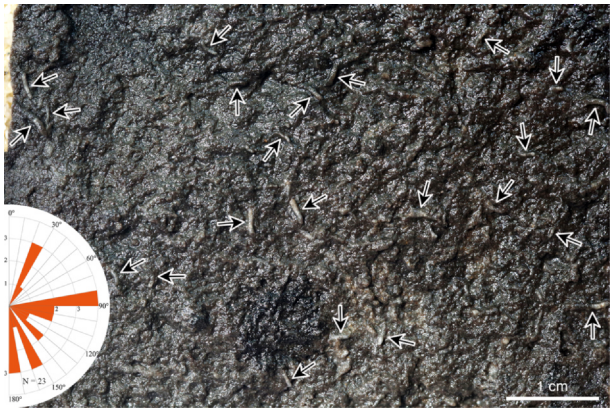

Fig. 9. Specimens of tubular fossils (arrows) exposed on bedding surface. Rose diagram on lower left shows a weak preferred orientation of the long axis of tubular fossils. N = 23 specimens. Museum catalog number: GEONWU-2019-BST007.

in eastern Yunnan (stratigraphically equivalent to the Shibantan and Gaojiashan members of the middle Dengying Formation; Yang et al., 2017a), a 545.76 ± 0.66 Ma age from the Liuchapo Formation in western Hunan (roughly equivalent to the Dengying Formation; Yang et al., 2017b), and the 536.40 ± 0.47 Ma and 541.48 ± 0.46 Ma ages from the Liuchapo Formation in eastern Guizhou (Wang et al., 2020).

Outside China, the *Cloudina–Sinotubulites* assemblage has been reported from the La Ciénega Formation in Mexico (McMenamin, 1985; Sour-Tovar et al., 2007) and the Ibor Group in central Spain (Cortijo et al., 2015b). The *Cloudina–Sinotubulites* assemblage, relative to *Cloudina* alone, is considered a more robust biostratigraphic indicator for the terminal Ediacaran stage, given that *Cloudina* may extend to the basal Cambrian (Yang et al., 2016; Zhu et al., 2017) but *Sinotubulites* is restricted to the terminal Ediacaran stage. Considering the available age constraints from South China and the likely age of ca. 539 Ma for the Ediacaran–Cambrian boundary (Linnemann et al., 2019), the *Cloudina–Sinotubulites* co-occurrence assemblage is constrained between ca. 551 Ma and ca. 539 Ma at a global scale.

The tubular fossils *Nevadatubulus dunfeei* and *Sinotubulites cienegensis* have been reported from the Deep Spring Formation in the White-Inyo Mountains of eastern California and in Esmeralda County, Nevada (Signor et al., 1987). While *Nevadatubulus dunfeei* is likely cogeneric with *Cloudina* (Grant, 1990) and has been synonymized with *Cloudina hartmannae* (Chen and Sun, 2001; Grant, 1990; Yang et al., 2016), the identification of *Sinotubulites* from the Deep Spring Formation is problematic because the illustrated specimen (Fig. 5.1 of Signor et al., 1987) is a conical rather than a cylindrical tube that is characteristic of *Sinotubulites*. Subsequent studies were unable to recover any unambiguous specimens of *Sinotubulites* from the Deep Spring Formation (Shuhai Xiao and Morrison Nolan, personal observation; James Schiffbauer and Emmy Smith, personal communications). Although it is expected that the *Cloudina–Sinotubulites* assemblage would occur in the Deep Spring Formation, which is likely of terminal Ediacaran in age (Smith et al., 2016), further investigation is needed to confirm this expectation.

6. Conclusions

We report the discovery of *Cloudina* from the terminal Ediacaran Baimatuo Member of the Dengying Formation in the Yangtze Gorges area of South China. *Cloudina* and other tubular fossils (including *Sinotubulites*) in the Baimatuo Member are secondarily silicified, a taphonomic mode that is also responsible for the preservation of *Cloudina* and *Sinotubulites* fossils in the Ibor Group of central Spain (Cortijo et al., 2015b). Thus far, the *Cloudina–Sinotubulites* co-occurrence assemblage has been reported from the Baimatuo Member (and possibly the Shibantan Member) of the Dengying Formation in the Yangtze Gorges area of South China, the Beiwan Member of the Dengying Formation in the Ningqiang area of southern Shaanxi Province of South China, the Ibor Group of central Spain, and the La Ciénega Formation in Mexico. Available radiometric dates constrain the *Cloudina–Sinotubulites* assemblage between ca. 551 Ma and ca. 539 Ma. The co-occurrence of *Cloudina* and *Sinotubulites* offers an important biostratigraphic marker for the terminal Ediacaran stage.

CRediT authorship contribution statement

Dandan Liang: Data curation, Writing - original draft, Writing -

Table 1
Measurements of silicified tubular fossils from the terminal Ediacaran Baimatuo Member in the Yangtze Gorges area.

Species	Illustration	Museum catalog number	Length (mm)	Adapertural diameter (mm)	Adapical diameter (mm)	Diameter (mm)
C. ningqiangensis		GEONWU-2019-YCSX-401-05	5.0	1.6	0.6	N/A
C. ningqiangensis		GEONWU-2019-YCSX-404-09	8.3	1.9	1.4	N/A
C. ningqiangensis	Fig. 3C	GEONWU-2019-BST001-002	10.9	2.4	1.4	N/A
C. sp. Indet.	Fig. 3D	GEONWU-2019-BST001-003	8.9	1.6	0.8	N/A
C. hartmannae	Fig. 4A	GEONWU-2019-BST002-001	28.1	2.5	1.7	N/A
C. cf. carinata	Fig. 5B	GEONWU-2019-BST003-001	27.4	4.2	2.3	N/A
S. baimatuoensis		GEONWU-2019-YCSX-401-18	2.5	N/A	N/A	1
S. baimatuoensis		GEONWU-2019-YCSX-402-01	6.0	N/A	N/A	1.1
S. baimatuoensis		GEONWU-2019-YCSX-402-02	5.4	N/A	N/A	1.6
S. baimatuoensis		GEONWU-2019-YCSX-402-03	7.4	N/A	N/A	1.8
S. baimatuoensis		GEONWU-2019-YCSX-402-04	7.4	N/A	N/A	1.8
S. baimatuoensis		GEONWU-2019-YCSX-402-06	5.7	N/A	N/A	1.5
S. baimatuoensis		GEONWU-2019-YCSX-403-02	16.2	N/A	N/A	2.1
S. baimatuoensis		GEONWU-2019-YCSX-404-01	5.3	N/A	N/A	1.5
S. baimatuoensis		GEONWU-2019-YCSX-404-10	9.6	N/A	N/A	2.3
S. baimatuoensis	Fig. 3B	GEONWU-2019-BST001-001	8.8	N/A	N/A	2
Sinotubulites	Fig. 6	GEONWU-2019-BST001-006	19.4	N/A	N/A	2.5
Unnamed	Fig. 5C	GEONWU-2019-BST003-002	18.0	N/A	N/A	1.6
Unnamed	Fig. 5D	GEONWU-2019-BST003-003	22.1	N/A	N/A	2.3
Unnamed	Fig. 7A	GEONWU-2019-YCSX-404-03	4.9	1.5	0.8	N/A
Unnamed	Fig. 7B	GEONWU-2019-YCSX-403-01	14.4	N/A	N/A	1.8
Unnamed	Fig. 7C	GEONWU-2019-YCSX-402-05	11.4	N/A	N/A	1.6
Unnamed	Fig. 7D	GEONWU-2019-YCSX-404-04	6.7	N/A	N/A	0.8
Unnamed	Fig. 7E	GEONWU-2019-YCSX-404-07	8.4	N/A	N/A	0.8
Unnamed	Fig. 7F	GEONWU-2019-YCSX-404-06	10.0	N/A	N/A	0.9

review & editing; **Yaoping Cai:** Funding acquisition, Project administration, Writing - review; **Morrison Nolan:** Data curation; **Shuhai Xiao:** Project administration, Funding acquisition, Writing - review & editing.

Declaration of Competing Interest

The authors declare that they have no known competing financial interests or personal relationships that could have appeared to influence the work reported in this paper.

Acknowledgements

This work was supported by National Key Research and Development Program of China (No. 2017YFC0603101), National Natural Science Foundation of China (Nos. 41972013, 41890840, 41621003), Key Scientific and Technological Innovation Team Project in Shaanxi Province ("Sanqin" Team Project), Shaanxi Science and Technology Innovation Team Project (No. 2019TD-012), State Key Laboratory of Continental Dynamics Research Project (No. 201210128), and Strategic Priority Research Program of Chinese Academy of Sciences (No. XDB26000000). S.X. and M.N. were supported by U.S. National Science Foundation (EAR-2021207). We thank Tara Selly, Lucas Warren and an anonymous reviewer for critical review.

References

Adôrno, R.R., Walde, D.H.G., Erdtmann, B.D., Denezine, M., Cortijo, I., Carmo, D.A.D., Giorgioni, M., Ramos, M.E.A.F., Fazio, G., 2019. First occurrence of *Cloudina carinata* Cortijo et al., 2010 in South America, Tamengo Formation, Corumbá Group, upper Ediacaran of Midwestern Brazil. Estud. Geol. 75, e95. https://doi.org/10.3989/egeol.43587.550.

Amthor, J.E., Grotzinger, J.P., Schröder, S., Bowring, S.A., Ramezani, J., Martin, M.W., Matter, A., 2003. Extinction of *Cloudina* and *Namacalathus* at the Precambrian-Cambrian boundary in Oman. Geology 31, 431–434.

Cai, Y., Cortijo, I., Schiffbauer, J.D., Hua, H., 2017. Taxonomy of the late Ediacaran index fossil *Cloudina* and a new similar taxon from South China. Precambr. Res. 298, 146–156. https://doi.org/10.1016/j.precamres.2017.05.016.

Cai, Y., Hua, H., Schiffbauer, J.D., Sun, B., Yuan, X., 2014. Tube growth patterns and microbial mat-related lifestyles in the Ediacaran fossil *Cloudina*, Gaojiashan Lagerstätte, South China. Gondwana Res. 25, 1008–1018. https://doi.org/10.1016/j.gr.2012.12.027.

Cai, Y., Hua, H., Xiao, S., Schiffbauer, J.D., Li, P., 2010. Biostratinomy of the late Ediacaran pyritized Gaojiashan Lagerstätte from southern Shaanxi, South China: importance of event deposits. Palaios 25, 487–506. https://doi.org/10.2110/palo.2009.p09-133r.

Cai, Y., Hua, H., Zhuravlev, A.Y., Gámez Vintaned, J.A., Ivantsov, A.Y., 2011. Discussion of 'First finds of problematic Ediacaran fossil *Gaojiashania* in Siberia and its origin'. Geol. Mag. 148, 329–333. https://doi.org/10.1017/s0016756810000749.

Cai, Y., Xiao, S., Hua, H., Yuan, X., 2015. New material of the biomineralizing tubular fossil *Sinotubulites* from the late Ediacaran Dengying Formation, South China. Precambr. Res. 261, 12–24. https://doi.org/10.1016/j.precamres.2015.02.002.

Cai, Y., Xiao, S., Li, G., Hua, H., 2019. Diverse biomineralizing animals in the terminal Ediacaran Period herald the Cambrian Explosion. Geology 47, 380–384. https://doi.org/10.1130/G45949.1.

Chen, M., Chen, Y., Qian, Y., 1981. Some tubular fossils from Sinian-Lower Cambrian boundary sequences, Yangtze Gorge. Bull. Tianjin Inst. Geol. Mineral Resour. 3, 117–124 (In Chinese with English abstract).

Chen, X., Zhou, P., Zhang, B., Wei, K., Zhang, M., 2016. Lithostratigraphy, biostratigraphy, sequence stratigraphy and carbon isotope chemostratigraphy of the upper Ediacaran in Yangtze Gorges and their significance for chronostratigraphy. Geologyand Miner. Resour. South China 32, 87–105 (In Chinese with English abstract).

Chen, Z., Bengtson, S., Zhou, C., Hua, H., Yue, Z., 2008. Tube structure and original composition of *Sinotubulites*: shelly fossils from the late Neoproterozoic in southern Shaanxi, China. Lethaia 41, 37–45. https://doi.org/10.1111/j.1502-3931.2007.00040.x.

Chen, Z., Sun, W., 2001. Late Sinian (tubular) metazoan fossils: *Cloudina* and *Sinotubulites* from southern Shaanxi. Acta Micropalaeontol. Sinica 18, 180–202 (In Chinese with English abstract).

Chen, Z., Zhou, C., Xiao, S., Wang, W., Guan, C., Hua, H., Yuan, X., 2014. New Ediacara fossils preserved in marine limestone and their ecological implications. Sci. Rep. 4, 4180. https://doi.org/10.1038/srep04180.

Condon, D., Zhu, M., Bowring, S., Wang, W., Yang, A., Jin, Y., 2005. U-Pb ages from the Neoproterozoic Doushantuo Formation, China. Science 308, 95–98.

Cortijo, I., Cai, Y., Hua, H., Schiffbauer, J.D., Xiao, S., 2015a. Life history and autecology of an Ediacaran index fossil: development and dispersal of *Cloudina*. Gondwana Res. 28, 419–424. https://doi.org/10.1016/j.gr.2014.05.001.

Cortijo, I., Martí Mus, M., Jensen, S., Palacios, T., 2010. A new species of *Cloudina* from the terminal Ediacaran of Spain. Precambr. Res. 176, 1–10.

Cortijo, I., Mus, M.M., Jensen, S., Palacios, T., 2015b. Late Ediacaran skeletal body fossil assemblage from the Navalpino anticline, central Spain. Precambr. Res. 267, 186–195. https://doi.org/10.1016/j.precamres.2015.06.013.

Cui, H., Kaufman, A.J., Xiao, S., Peek, S., Cao, H., Min, X., Cai, Y., Siegel, Z., Liu, X., Peng, Y., Schiffbauer, J.D., Martin, A.J., 2016. Environmental context for the terminal Ediacaran biomineralization of animals. Geobiology 14, 344–363. https://doi.org/10.1111/gbi.12178.

Cui, H., Xiao, S., Cai, Y., Peek, S., Plummer, R.E., Kaufman, A.J., 2019. Sedimentological and chemostratigraphic investigations of the terminal Ediacaran Dengying Formation, Gaojiashan, South China. Geol. Mag. 156, 1924–1948. https://doi.org/10.1017/S0016756819000293.

Ding, Y., Chen, D., Zhou, X., Guo, C., Huang, T., Zhang, G., 2019. Tectono-depositional pattern and evolution of the middle Yangtze Platform (South China) during the late Ediacaran. Precambr. Res. 333, 105426. https://doi.org/10.1016/j.precamres.2019.105426.

Grant, S.W.F., 1990. Shell structure and distribution of *Cloudina*, a potential index fossil for the terminal Proterozoic. Am. J. Sci. 290-A, 261–294.

Grazhdankin, D.V., Kontorovich, A.E., Kontorovich, V.A., Saraev, S.V., Filippov, F. Yu., Efimov, A.S., Karlova, G.A., Kochnev, B.B., Nagovitsin, K.E., Terleev, A.A., Fedyanin, G.O., 2015. Vendian of the Fore-Yenisei sedimentary basin (southeastern West Siberia). Russ. Geol. Geophys. 56, 560–572. https://doi.org/10.1016/j.rgg.2015.03.008.

Hofmann, H.J., Mountjoy, E.W., 2001. *Namacalathus-Cloudina* assemblage in Neoproterozoic Miette Group (Byng Formation), British Columbia: Canada's oldest shelly fossils. Geology 29, 1091–1094.

Hua, H., Chen, Z., Yuan, X., 2007. The advent of mineralized skeletons in Neoproterozoic Metazoa: new fossil evidence from the Gaojiashan Fauna. Geol. J. 42, 263–279.

Hua, H., Chen, Z., Yuan, X., Zhang, L., Xiao, S., 2005. Skeletogenesis and asexual reproduction in the earliest biomineralizing animal *Cloudina*. Geology 33, 277–280. https://doi.org/10.1130/g21198.1.

Hua, H., Zhang, L., Zhang, Z., Wang, J., 2000. New fossil evidence from latest Neoproterozoic Gaojiashan biota, south Shaanxi. Acta Palaeontol. Sinica 39, 381–390 (In Chinese with English abstract).

Huang, T., Chen, D., Ding, Y., Zhou, X., Zhang, G., 2019. SIMS U-Pb zircon geochronological and carbon isotope chemostratigraphic constraints on the Ediacaran-Cambrian boundary succession in the Three Gorges Area, South China. J. Earth Sci. 31, 69–78. https://doi.org/10.1007/s12583-019-1233-x.

Kontorovich, A.E., Varlamov, A.I., Grazhdankin, D.V., Karlova, G.A., Klets, A.G., Kontorovich, V.A., Saraev, S.V., Terleev, A.A., Belyaev, S.Y., Varaksina, I.V., Efimov, A.S., Kochnev, B.B., Nagovitsin, K.E., Postnikov, A.A., Filippov, Y.F., 2008. A section of Vendian in the east of West Siberian Plate (based on data from the Borehole Vostok 3). Russ. Geol. Geophys. 49, 932–939.

Linnemann, U., Ovtcharova, M., Schaltegger, U., Gärtner, A., Hautmann, M., Geyer, G., Vickers-Rich, P., Rich, T., Plessen, B., Hofmann, M., Zieger, J., Krause, R., Kriesfeld, L., Smith, J., 2019. New high-resolution age data from the Ediacaran-Cambrian boundary indicate rapid, ecologically driven onset of the Cambrian explosion. Terra Nova 31, 49–58. https://doi.org/10.1111/ter.12368.

Maliva, R.G., Knoll, A.H., Simonson, B.M., 2005. Secular change in the Precambrian silica cycle: insights from chert petrology. Geol. Soc. Am. Bull. 117, 835–845.

McMenamin, M.A.S., 1985. Basal Cambrian small shelly fossils from the La Ciénega Formation, northwestern Sonora, Mexico. J. Paleontol. 59, 1414–1425.

Mehra, A., Maloof, A., 2018. Multiscale approach reveals that *Cloudina* aggregates are detritus and not *in situ* reef constructions. Proc. Natl. Acad. Sci. U.S.A. 115, E2519–E2527. https://doi.org/10.1073/pnas.1719911115.

Meyer, M., Xiao, S., Gill, B.C., Schiffbauer, J.D., Chen, Z., Zhou, C., Yuan, X., 2014. Interactions between Ediacaran animals and microbial mats: insights from *Lamonte trevallis*, a new trace fossil from the Dengying Formation of South China. Palaeogeogr. Palaeoclimatol. Palaeoecol. 396, 62–74. https://doi.org/10.1016/j.palaeo.2013.12.026.

Penny, A.M., Wood, R.A., Curtis, A., Bowyer, F., Tostevin, R., Hoffmann, K.H., 2014. Ediacaran metazoan reefs from the Nama Group, Namibia. Science 344, 1504–1506.

Signor, P.W., Mount, J.F., Onken, B.R., 1987. A pre-trilobite shelly fauna from the White-Inyo region of eastern California and western Nevada. J. Paleontol. 61, 425–438.

Smith, E.F., Nelson, L.L., Strange, M.A., Eyster, A.E., Rowland, S.M., Schrag, D.P., Macdonald, F.A., 2016. The end of the Ediacaran: two new exceptionally preserved body fossil assemblages from Mount Dunfee, Nevada, USA. Geology 44, 911–914. https://doi.org/10.1130/G38157.1.

Sour-Tovar, F., Hagadorn, J.W., Huitrón-Rubio, T., 2007. Ediacaran and Cambrian index fossils from Sonora, Mexico. Palaeontology 50, 169–175.

Walde, D.H.G., Weber, B., Erdtmann, B.D., Steiner, M., 2019. Taphonomy of *Corumbella werneri* from the Ediacaran of Brazil: sinotubulitid tube or conulariid test? Alcheringa 43, 335–350. https://doi.org/10.1080/03115518.2019.1615551.

Wang, W., Zhou, M., Chu, Z., Xu, J., Li, C., Luo, T., Guo, J., 2020. Constraints on the Ediacaran-Cambrian boundary in deep-water realm in South China: evidence from zircon CA-ID-TIMS U-Pb ages from the topmost Liuchapo Formation. Sci. China Earth Sci. https://doi.org/10.1007/s11430-019-9590-0.

Warren, L.V., Fairchild, T.R., Gaucher, C., Boggiani, P.C., Poiré, D.G., Anelli, L.E., Inchausti, J.C.G., 2011. *Corumbella* and *in situ Cloudina* in association with thrombolites in the Ediacaran Itapucumi Group, Paraguay. Terra Nova 23, 382–389. https://doi.org/10.1111/j.1365-3121.2011.01023.x.

Warren, L.V., Quaglio, F., Simões, M.G., Gaucher, C., Riccomini, C., Poiré, D.G., Freitas, B.T., Boggiani, P.C., Sial, A.N., 2017. *Cloudina–Corumbella–Namacalathus* association

from the Itapucumi Group, Paraguay: increasing ecosystem complexity and tiering at the end of the Ediacaran. Precambr. Res. 298, 79–87. https://doi.org/10.1016/j.precamres.2017.05.003.
Wood, R., 2016. Palaeoecology of Ediacaran metazoan reefs. Geol. Soc. London Spec. Publ. 448, 195–210. https://doi.org/10.1144/SP448.1.
Wood, R., Curtis, A., 2015. Extensive metazoan reefs from the Ediacaran Nama Group, Namibia: the rise of benthic suspension feeding. Geobiology 13, 112–122. https://doi.org/10.1111/gbi.12122.
Wood, R., Ivantsov, A.Y., Zhuravlev, A.Y., 2017. First macrobiota biomineralization was environmentally triggered. Proc. R. Soc. B (Biol. Sci.) 284, 20170059. https://doi.org/10.1098/rspb.2017.0059.
Xiao, S., Narbonne, G.M., 2020. The Ediacaran period. In: Gradstein, F.M., Ogg, J.G., Schmitz, M., Ogg, G. (Eds.), Geological Time Scale 2020. Elsevier, Oxford in press.
Xiao, S., Schiffbauer, J.D., McFadden, K.A., Hunter, J., 2010. Petrographic and SIMS pyrite sulfur isotope analyses of Ediacaran chert nodules: implications for microbial processes in pyrite rim formation, silicification, and exceptional fossil preservation. Earth Planet. Sci. Lett. 297, 481–495. https://doi.org/10.1016/j.epsl.2010.07.001.
Yang, B., Steiner, M., Schiffbauer, J.D., Selly, T., Wu, X., Zhang, C., Liu, P., 2020. Ultrastructure of Ediacaran cloudinids suggests diverse taphonomic histories and affinities with non-biomineralized annelids. Sci. Rep. 10, 535. https://doi.org/10.1038/s41598-019-56317-x.
Yang, B., Steiner, M., Zhu, M., Li, G., Liu, J., Liu, P., 2016. Transitional Ediacaran-Cambrian small skeletal fossil assemblages from South China and Kazakhstan: implications for chronostratigraphy and metazoan evolution. Precambr. Res. 285, 202–215. https://doi.org/10.1016/j.precamres.2016.09.016.
Yang, C., Li, X.-H., Zhu, M., Condon, D.J., 2017a. SIMS U-Pb zircon geochronological constraints on upper Ediacaran stratigraphic correlations, South China. Geol. Mag. 154, 1202–1216. https://doi.org/10.1017/S0016756816001102.
Yang, C., Zhu, M., Condon, D.J., Li, X.H., 2017b. Geochronological constraints on stratigraphic correlation and oceanic oxygenation in Ediacaran-Cambrian transition in South China. J. Asian Earth Sci. 140, 75–81. https://doi.org/10.1016/j.jseaes.2017.03.017.
Zhang, L., Dong, J., Tian, S., Ding, L., 1992. The Gaojiashan biota. In: Ding, L., Zhang, L., Li, Y., Dong, J. (Eds.), The Study of the Late Sinian–Early Cambrian Biotas from the Northern Margin of the Yangtze Platform. Scientific and Technical Documents Publishing House, Beijing, pp. 33–63 (In Chinese with English summary).
Zhao, J.H., Zhou, M.F., Zheng, J.P., 2013. Neoproterozoic high-K granites produced by melting of newly formed mafic crust in the Huangling region, South China. Precambr. Res. 233, 93–107. https://doi.org/10.1016/j.precamres.2013.04.011.
Zhou, C., Xiao, S., 2007. Ediacaran $\delta^{13}C$ chemostratigraphy of South China. Chem. Geol. 237, 89–108.
Zhu, M., Zhuravlev, A.Y., Wood, R.A., Zhao, F., Sukhov, S.S., 2017. A deep root for the Cambrian Explosion: implications of new bio- and chemostratigraphy from the Siberian Platform. Geology 45, 459–462. https://doi.org/10.1130/G38865.1.
Zhuravlev, A., Liñán, E. Yu., Vintaned, J.A.G., Debrenne, F., Fedorov, A.B., 2012. New finds of skeletal fossils in the terminal Neoproterozoic of the Siberian Platform and Spain. Acta Palaeontol. Pol. 57, 205–224. https://doi.org/10.4202/app.2010.0074.